Check for updates

Rapid, high-sensitivity analysis of oxyhalides by non-suppressed ion chromatography-electrospray ionization-mass spectrometry: application to ClO_4^-, ClO_3^-, ClO_2^-, and BrO_3^- quantification during sunlight/chlorine advanced oxidation†

Tessora R. Young, [ID] [a] Shi Cheng,[b] Wentao Li[b] and Michael C. Dodd [ID] *[a]

A rapid and sensitive method is described for measuring perchlorate (ClO_4^-), chlorate (ClO_3^-), chlorite (ClO_2^-), bromate (BrO_3^-), and iodate (IO_3^-) ions in natural and treated waters using non-suppressed ion chromatography with electrospray ionization and tandem mass spectrometry (NS-IC-MS/MS). Major benefits of the NS-IC-MS/MS method include a short analysis time (12 minutes), low limits of quantification for BrO_3^- (0.10 μg L^{-1}), ClO_4^- (0.06 μg L^{-1}), ClO_3^- (0.80 μg L^{-1}), and ClO_2^- (0.40 μg L^{-1}), and compatibility with conventional LC-MS/MS instrumentation. Chromatographic separations were generally performed under isocratic conditions with a Thermo Scientific Dionex AS16 column, using a mobile phase of 20% 1 M aqueous methylamine and 80% acetonitrile. The isocratic method can also be optimized for IO_3^- analysis by including a gradient from the isocratic mobile phase to 100% 1 M aqueous methylamine. Four common anions (Cl$^-$, Br$^-$, SO_4^{2-}, and HCO_3^-/CO_3^{2-}), a natural organic matter isolate (Suwannee River NOM), and several real water samples were tested to examine influences of natural water constituents on oxyhalide detection. Only ClO_2^- quantification was significantly affected – by elevated chloride concentrations (>2 mM) and NOM. The method was successfully applied to quantify oxyhalides in natural waters, chlorinated tap water, and waters subjected to advanced oxidation by sunlight-driven photolysis of free available chlorine (sunlight/FAC). Sunlight/FAC treatment of NOM-free waters containing 200 μg L^{-1} Br$^-$ resulted in formation of up to 263 ± 35 μg L^{-1} and 764 ± 54 μg L^{-1} ClO_3^-, and up to 20.1 ± 1.0 μg L^{-1} and 33.8 ± 1.0 μg L^{-1} BrO_3^- (at pH 6 and 8, respectively). NOM strongly inhibited ClO_3^- and BrO_3^- formation, likely by scavenging reactive oxygen or halogen species. As prior work shows that the greatest benefits in applying the sunlight/FAC process for purposes of improving disinfection of chlorine-resistant microorganisms are realized in waters with lower DOC levels and higher pH, it may therefore be desirable to limit potential applications to waters containing moderate DOC concentrations (*e.g.*, ~1–2 mg$_C$ L^{-1}), low Br$^-$ concentrations (*e.g.*, <50 μg L^{-1}), and circumneutral to moderately alkaline pH (*e.g.*, pH 7–8) to strike a balance between maximizing microbial inactivation while minimizing formation of oxyhalides and other disinfection byproducts.

Water impact

A novel NS-IC-MS/MS method enables rapid, highly-sensitive quantification of all regulated oxyhalides using widely-available LC-MS instrumentation in place of highly-specialized suppressed IC-MS platforms. The method provides sub-μg L^{-1} sensitivities in analyses of natural and treated water matrixes, and can provide a simple, accessible means for monitoring oxyhalides in water resources and during advanced oxidative treatment, as demonstrated using sunlight-driven chlorine photolysis.

[a] Dept. of Civil and Environmental Engineering, University of Washington, 305 More Hall, Box 352700, Seattle, WA 98195-2700, USA.
E-mail: tessora.young@kubota.com, doddm@uw.edu; Fax: +206 543 1543;
Tel: +206 685 7583
[b] State Key Laboratory of Pollution Control and Resources Reuse, School of the Environment, Nanjing University, Nanjing, 210023, China.
E-mail: shicheng_nju@163.com, liwentao@nju.edu.cn
† Electronic supplementary information (ESI) available. See DOI: 10.1039/d0ew00429d

Introduction

Alternative oxidants, such as ozone (O_3) and chlorine dioxide (ClO_2), are frequently used in (waste)water treatment to oxidize organic contaminants and improve disinfection of chlorine resistant pathogens while satisfying regulatory targets for halogenated organic disinfection byproducts (DBPs).[1,2] However, the use of O_3 and ClO_2 can lead to

2580 | *Environ. Sci.: Water Res. Technol.*, 2020, **6**, 2580–2596

This journal is © The Royal Society of Chemistry 2020

formation of significant concentrations of regulated and unregulated oxyhalide DBPs.[3–5] Additionally, as a majority of utilities have discontinued using chlorine gas (90% in 1978 to 40% in 2017) as a source of free available chlorine (FAC) and transitioned to sodium hypochlorite (NaOCl) solutions (56% in 2017) or onsite FAC generation to reduce safety hazards and security risks associated with chlorine gas storage and transport,[6] oxyhalide formation has also become an increasing concern for utilities employing chlorine.[7] For example, concentrated NaOCl stocks and on-site generated FAC often contain perchlorate (ClO_4^-), chlorate (ClO_3^-), chlorite (ClO_2^-), and bromate (BrO_3^-) as contaminants, and are potentially significant sources of these oxyhalides in finished water.[7–11]

The U.S. Environmental Protection Agency (EPA) enforces maximum contaminant levels (MCLs)[12] of 10 μg L^{-1} for BrO_3^- (a probable human carcinogen[13]), and 1.0 mg L^{-1} for ClO_2^- (which has been shown to decrease red blood cells and hemoglobin[14]). Currently there are not enforceable MCLs for ClO_3^- or ClO_4^- in drinking water; however, the U.S. EPA has set a health reference level[15] of 210 μg L^{-1} for ClO_3^- (which – like ClO_2^- – has been shown to decrease red blood cells and hemoglobin[14,16]) and a proposed MCL[17] of 56 μg L^{-1} for ClO_4^- (which can interfere with iodide uptake and thyroid activity[18]).

With increasing usage of alternative disinfection strategies in water treatment, the monitoring of inorganic oxyhalide DBPs introduced from disinfectant stocks or formed during oxidation/disinfection processes is a concern for utilities and regulatory agencies worldwide. Furthermore, growing interest

in the application of novel advanced oxidation processes based on the photolysis of FAC (e.g., UV/chlorine[19–23] and sunlight/chlorine[24–26]) – especially in the context of potable water reuse – also provide substantial motivation for the continued advancement of methods for rapid, sensitive, simple, and accessible oxyhalide analyses.

A wide range of standards and published methods have been developed for the analyses of oxyhalides – generally employing either ion chromatography (IC) or liquid chromatography (LC), with a range of detection methods encompassing conductivity, post-column reaction with UV/visible absorbance detection, mass spectrometry (MS), and inductively coupled plasma-mass spectrometry (ICP-MS).[27] Selected details and limits of detection (LODs) for a cross-section of reported methods for analyses of ClO_2^-, ClO_3^-, ClO_4^-, BrO_3^-, and iodate (IO_3^-, which is also a common, unregulated byproduct generated during oxidative treatment of iodide-containing waters[28]) are summarized in Table 1.

Each of the oxyhalides can be detected by conventional IC utilizing suppressed conductivity detection, though such approaches typically require pre-concentration or post-column reactions to achieve sub-μg L^{-1} quantification, and often require use of multiple methods and/or columns to enable quantification of all oxyhalides. One- and two-dimensional-IC with use of various post-column reactions can enable excellent chromatographic resolution and high-sensitivity analyses of ClO_2^-, BrO_3^-, and IO_3^-.[29–36] However, few post-column reaction methods are optimized for ClO_3^- analysis,[37,38] and ClO_4^- is not typically amenable to such approaches. IC-MS/MS methods have been utilized to achieve

Table 1 Cross-section of representative methods reported for the analyses of oxyhalides using various analytical approaches with accompanying limits of detection

Analysis approach[a]	ClO_4^- μg L^{-1}	ClO_3^- μg L^{-1}	ClO_2^- μg L^{-1}	BrO_3^- μg L^{-1}	IO_3^- μg L^{-1}	Reference
IC-Conductivity	—	1.3	0.9	1.4	—	46
IC-Conductivity	1.0	0.6	—	0.6	1.4	44
2D IC-conductivity	—	—	—	0.18	—	30
2D IC-conductivity	0.06	—	—	—	—	32
IC-PCR-UV/vis	—	0.92	0.45	0.12	—	47
IC-PCR-UV/vis	—	—	—	0.17	—	31
IC-PCR-UV/vis	—	—	—	0.1	<2.0	29
IC-PCR-UV/vis	—	—	—	—	0.1	48
IC-MS	—	—	—	0.07	—	42
IC-MS	10	9	—	39	22	44
IC-MS/MS	0.0005	—	—	—	—	40
IC-MS/MS	0.02	—	—	—	—	39
IC-MS/MS	—	—	—	0.02	—	41
IC-MS/MS	—	—	—	0.005	—	45
LC-MS/MS	0.006	0.23	—	0.058	—	49
LC-MS/MS	0.022	0.045	—	0.049	0.069	50
NS-IC-MS/MS	0.02	—	—	—	—	51
NS-IC-MS/MS	0.04	—	—	0.01	—	52
NS-IC-MS/MS	—	—	—	0.01	0.02	53
NS-IC-MS/MS	0.003	—	—	—	—	54
NS-IC-ICP/MS				1.65	0.33	55

[a] Analysis abbreviations: ion chromatography (IC), two-dimensional ion chromatography (2D IC), post-column reaction with UV/visible light absorbance detection (PCR-UV/vis), non-suppressed (NS), mass spectrometry (MS), tandem mass spectrometry (MS/MS), and inductively coupled plasma (ICP).
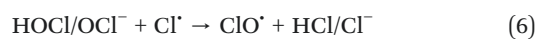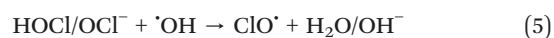
high chromatographic resolutions and sensitivities in the analyses of each of the regulated oxyhalides.[39–45] However, the use of an organic mobile phase modifier such as acetonitrile or methanol is often required (either *via* post-suppressor infusion into the MS, or as part of the mobile phase) to achieve optimal analyte sensitivities (in particular for ClO_4^-).[39,40,43,44] Furthermore, conventional IC separation with KOH or NaOH as hydroxide sources requires use of an ion suppressor before MS detection, necessitating the use of specialized IC instrumentation.

In several alternative approaches, volatile mobile phase counter-ion sources such as methylamine or ammonium nitrate have been employed in place of KOH or NaOH to enable the use of IC-MS or IC-ICP-MS detection without the need for an ion suppressor,[52–57] with a number of these enabling rapid, selective, and sensitive non-suppressed-IC-MS/MS (NS-IC-MS/MS) analyses of ClO_4^-, BrO_3^-, and IO_3^- on conventional LC and MS systems (Table 1).[43,51,53] Reversed-phase LC-MS/MS methods using mobile phases comprising acetonitrile with various volatile aqueous buffers (*e.g.*, formic acid, ammonium formate, or ammonium acetate) have also been applied for rapid, high sensitivity analyses of ClO_4^-, ClO_3^-, BrO_3^-, and IO_3^- without an ion suppressor.[49,50,58]

In a particularly intriguing approach that incorporated many of the uniquely advantageous features of the methods described above, Charles and Pepin (1998) utilized a combination of a high proportion of organic mobile phase modifier (90% methanol) and a volatile counter-ion source (50 mg L^{-1} ammonium nitrate) with a low-capacity AG9-SC guard column to achieve rapid (<12 min), isocratic, sub-µg L^{-1} sensitivity detection of ClO_3^-, ClO_2^-, BrO_3^-, and IO_3^- using NS-IC-MS/MS, though the chromatographic resolution of the AG9-SC column was limited, and their method was not optimized for ClO_4^-.[57]

Drawing on the compelling advantages of the latter approach (*i.e.*, speed, simplicity, high sensitivity, use of conventional LC-MS instrumentation), this work investigated the development and application of a novel method employing an acetonitrile and water mobile phase with methylamine as a hydroxide source to enable rapid, high-sensitivity analysis of all five of the oxyhalides most relevant to (waste)water treatment – ClO_2^-, ClO_3^-, ClO_4^-, BrO_3^-, and IO_3^- – by NS-IC-MS/MS. This method eliminates the need for an ion suppressor – allowing the use of conventional LC-MS instrumentation – and enables highly sensitive routine detection of ClO_2^-, ClO_3^-, ClO_4^-, and BrO_3^-, with a minor modification enabling IO_3^- analysis. The new NS-IC-MS/MS method was validated by: (a) evaluating the effects of common water matrix constituents – including Cl^-, Br^-, SO_4^{2-}, HCO_3^-/CO_3^{2-}, and natural organic matter (NOM) – on signal intensities and retention times of oxyhalides spiked into high purity reagent water, and by (b) quantifying oxyhalide concentrations in (i) several natural water matrixes spiked with each oxyhalide, (ii) a tap water originating from a treatment facility employing ozone and chlorine disinfection, and (iii) NaOCl stocks.

The NS-IC-MS/MS method was then applied to quantify oxyhalide formation and/or loss during the solar irradiation of FAC-containing waters (sunlight/FAC), which has recently been evaluated as a novel advanced oxidation and disinfection process for drinking water treatment.[24,26,59,60] Sunlight/FAC treatment produces various reactive oxygen and halogen species and other oxidants *in situ* (*e.g.*, O_3, ˙OH, Cl˙, ClO˙, $Cl_2^{˙-}$ as shown in eqn (1)–(7) and Table S1†),[23,61–65]

$$HOCl \overset{hv}{\rightarrow} \, ˙OH + Cl˙ \tag{1}$$

$$OCl^- \overset{hv}{\rightarrow} O^{˙-} + \, Cl˙ \tag{2}$$

$$OCl^- \overset{hv}{\rightarrow} O(^3P) + Cl^- \tag{3}$$

$$O(^3P) + O_2 \rightarrow O_3 \tag{4}$$

$$HOCl/OCl^- + ˙OH \rightarrow ClO˙ + H_2O/OH^- \tag{5}$$

$$HOCl/OCl^- + Cl˙ \rightarrow ClO˙ + HCl/Cl^- \tag{6}$$

$$Cl^- + Cl˙ \rightarrow Cl_2^{˙-} \tag{7}$$

which are known to contribute to formation of oxyhalides, including ClO_2^-, ClO_3^-, and ClO_4^-, in addition to BrO_3^- if Br^- is present.[22,66,67] Oxyhalide formation has previously been observed at high levels during sunlight- or UVA-driven photolysis of FAC and free available bromine in various systems. For example, BrO_3^- has been detected at concentrations reaching ~100 µg L^{-1} in open chlorinated drinking water reservoirs during exposure of impounded water to natural sunlight, and at concentrations up to several mg L^{-1} in seawater amended with 4–5 mg L^{-1} as Cl_2 of FAC following bench-scale exposure to several hours of natural sunlight.[68,69] ClO_3^- and ClO_4^- have been detected at respective concentrations reaching several hundred mg L^{-1} and several tens of µg L^{-1} in concentrated (>100 mg L^{-1} as Cl_2) FAC stock solutions exposed to several hours of high-intensity UVB or UVA irradiation.[67] However, in recent work examining the use of sunlight/FAC treatment to degrade various trace organic contaminants under milder conditions (*e.g.*, exposure of 8 mg L^{-1} as Cl_2 to 15 minutes of solar irradiation), only ClO_3^- was reported to exceed detection limits (at levels reaching ~600 µg L^{-1}), though this may have been in part due to relatively low method sensitivities for ClO_2^- and BrO_3^-.[24,26] Thus, in the present work, the NS-IC-MS/MS method was used to further investigate the extent to which ClO_2^-, ClO_3^-, ClO_4^-, and BrO_3^- form during application of this novel treatment process to artificial and natural drinking water matrixes under milder, controlled conditions.

Experimental materials and methods

Materials

$NaBrO_3$ (>99%), $NaClO_3$ (>99%), $NaClO_2$ (80%), and KIO_3 (>99.5%) were obtained from Sigma-Aldrich (St. Louis, MO).

NaClO$_4$ (>98%) was obtained from EMD (Darmstadt, Germany). Isotope-labeled perchlorate (Cl^{18}O$_4^-$) and bromate (Br^{18}O$_3^-$) were obtained from Icon Isotopes (Summit, NJ) and isotope-labeled chlorate (Cl^{18}O$_3^-$) was obtained from EU Reference Laboratories (Stuttgart, Germany). Mass spectrometry grade water and CHROMASOLV acetonitrile; methylamine (40% in water); NaOCl (reagent grade, 4.00–4.99% in water); ethylene diamine (>99%); and NaCl, NaBr, Na$_2$SO$_4$, Ba(OH)$_2$, NaH$_2$PO$_4$, and Na$_2$HPO$_4$ (ACS reagent grade or higher) were all obtained from Sigma-Aldrich (St. Louis, MO). Suwannee River natural organic matter (SRNOM; reverse-osmosis isolate 2R101N), was obtained from the International Humic Substances Society (St. Paul, MN). All aqueous stock and calibration standards were prepared in Milli-Q water with resistivity ≥18.2 MΩ cm (Millipore, Billerica, MA).

Safety considerations. Methylamine is a highly volatile and flammable chemical that can cause respiratory irritation and toxicity, eye damage, and severe skin burns at high concentrations. Review supplier safety data sheets before use. Appropriate PPE should be worn during handling to provide eye and skin protection, stock solutions should be prepared in a fume hood, and mobile phase bottles containing methylamine solutions should be tightly sealed to prevent its volatilization into the ambient air during use.

Sample collection and storage

Natural samples and SRNOM stocks were filtered using 0.45 μm polyethersulfone membranes (conditioned by flushing with 1 L of Milli-Q water) prior to storage at 4 °C in carbon-free glassware (pre-baked at 400 °C). Tap water was collected from a public restroom after flushing the faucet with cold water for 2 minutes prior to sample collection. Residual FAC in the tap water was sequestered with 0.12 mM ethylene diamine (EDA), and the sample filtered as above prior to analyses. FAC residual in the tap water was estimated as 0.6 mg L^{-1} as Cl$_2$ by measuring the total available chlorine (TAC) attributable to the N-chloramine(s) resulting from reaction of FAC with EDA, using DPD colorimetry.[70]

EDA is a widely-used FAC quenching reagent that functions as a preservative for ClO$_2^-$ and is compatible with the other oxyhalides,[11,71–73] and is recommended for the preservation of samples in U.S. EPA standard methods for oxyhalides.[46,47] EDA is also not anticipated to interfere with either chromatography or post-column detection of the oxyhalides in the current method, as neither its positively charged nor neutral forms should be retained by the AS16 column, and will thus not co-elute with any of the oxyhalides.

Instrumentation

Three LC-MS/MS systems were used in this work: System 1 – a Shimadzu LC-20AD binary HPLC equipped with an SPD-20A UV/vis detector (not used) and interfaced with an AB Sciex API 4000 QTRAP linear ion trap with hybrid triple-quadrupole mass spectrometer (AB Sciex, Framingham, MA) – used for all but IO$_3^-$ analyses; System 2 – a Waters Acquity UPLC H Class Quaternary HPLC also interfaced with an AB Sciex API 4000 QTRAP mass spectrometer – used to investigate gradient analyses of IO$_3^-$; and System 3 – an Agilent 1290 HPLC system coupled with an AB Sciex QTRAP 5500 linear ion trap with hybrid triple-quadrupole mass spectrometer (AB Sciex, Framingham, MA) – used to investigate isocratic analyses of IO$_3^-$. In each case, the HPLC systems delivered varying proportions of 1 M aqueous methylamine (eluent "A") and acetonitrile (eluent "B") through the column to the mass spectrometer at a flow rate of 0.25 mL min^{-1}. Eluents A and B were separated to prevent alkaline hydrolysis of acetonitrile during storage.[74] Samples were analyzed using injection volumes of either 10 or 100 μL, with analytes separated using a 250 × 2 mm Thermo Scientific Dionex IonPac® AS16 hydroxide selective column (9 μm particle size and 2000 Å pore size) with an AG16 guard column (Bannockburn, IL).

Mass spectrometry

Mass spectrometry was undertaken using negative mode electrospray ionization (ESI) with the following parameters: 20 psig nebulizer gas, 30 psig turbo gas, −4500 V ion spray voltage, 400 °C source temperature, and 40 psig curtain gas. Oxyhalide identities were confirmed using naturally occurring chlorine and bromine isotopes, with chlorine masses of 34.969 Da (75.78% abundance) and 36.966 Da (24.22% abundance) and bromine masses of 78.91 Da (50.69% abundance) and 80.91 Da (49.31% abundance), and selected reaction monitoring (SRM) with the analyte-specific precursor/product ion transitions and detector settings shown in Table 2.

ClO$_4^-$, ClO$_3^-$, and BrO$_3^-$ were quantified using the respective ^{18}O-isotope labeled internal standards, ^{35}Cl^{18}O$_4^-$, ^{35}Cl^{18}O$_4^-$ or ^{35}Cl^{18}O$_3^-$, and ^{81}Br^{18}O$_3^-$ – each spiked to all

Table 2 Compound-specific selected reaction monitoring (SRM) MS/MS parameters for oxyhalide ions, optimized *via* direct infusion in 20% A + 80% B

Compound	Precursor ion mass (m/z)	Product ion mass (m/z)	Collision energy (volts)	Collision cell exit potential (volts)
^{81}BrO$_3^-$	128.88	113.00	−34.0	−9.0
^{79}BrO$_3^-$	126.88	110.80	−48.0	−7.0
^{37}ClO$_4^-$	101.05	84.80	−34.0	−13.0
^{35}ClO$_4^-$	99.02	83.10	−34.0	−13.0
^{37}ClO$_3^-$	84.97	69.10	−34.0	−9.0
^{35}ClO$_3^-$	82.96	67.00	−28.0	−10.0
^{37}ClO$_2^-$	69.01	53.00	−20.0	−7.0
^{35}ClO$_2^-$	67.00	50.90	−18.0	−7.0
^{81}Br^{18}O$_3^-$	135.00	116.90	−30.0	−17.0
^{79}Br^{18}O$_3^-$	132.90	114.90	−32.0	−17.0
^{37}Cl^{18}O$_4^-$	109.01	91.00	−36.0	−13.0
^{35}Cl^{18}O$_4^-$	107.00	89.00	−38.0	−13.0
^{37}Cl^{18}O$_3^-$	90.975	73.000	−28.0	−5.0
^{35}Cl^{18}O$_3^-$	89.00	71.00	−28.0	−5.0
IO$_3^-$	174.70	158.70	−38.0	−14.0

This journal is © The Royal Society of Chemistry 2020

Environ. Sci.: Water Res. Technol., 2020, **6**, 2580–2596 | **2583**

samples at 10 μg L^{-1}. No ^{18}O-isotope labeled standard was commercially-available for ClO$_2^-$, so ClO$_2^-$ was quantified using the ^{35}Cl^{18}O$_4^-$ internal standard. Concentrations for all oxyhalides were determined from external calibration curves of oxyhalide standards diluted in Milli-Q water, with normalization of external standard peak areas to the corresponding peak areas of the appropriate 10 μg L^{-1} ^{18}O-isotope labeled internal standards. Standard calibrations were run either (a) individually for each pair of external and internal oxyhalide standards prepared in Milli-Q water, or (b) in mixtures of ClO$_4^-$, ClO$_3^-$, and BrO$_3^-$ amended with associated internal standards in Milli-Q water, with separate ClO$_2^-$ calibration standards run in Milli-Q water due to the presence of ClO$_3^-$ as a contaminant of the NaClO$_2$ stock (Fig. S1†). Collision energies and collision cell exit potentials for each analyte were optimized via direct infusion of oxyhalide standards, using the auto-tuning function in the Analyst instrument control software, and are listed in Table 2.

Dark chlorination and sunlight/FAC experiments

In order to facilitate comparison with prior work, experiments were undertaken at temperature, FAC, pH, and fluence levels representative of conditions utilized in previous studies on sunlight/FAC treatment.[24,26,59,60] Dark chlorination experiments (FAC only) were conducted in amber glass reactors and thermostated at 10 °C via a water bath connected to a recirculating chiller. Sunlight/FAC experiments were run in duplicate in 28 mL quartz tubes and also thermostated at 10 °C via a water bath connected to a recirculating chiller located within the solar simulator. The quartz tubes containing sunlight/FAC reaction solutions were irradiated using an Atlas XPS+ solar simulator with a 1700 W, O$_3$-free, Xe arc lamp equipped with a daylight filter (cutoff below 290 nm) and infrared radiation filter, with spectral irradiance as shown in Fig. S2.† Ten mM phosphate buffer was used to maintain pH in buffered samples at either 6.0 or 8.0 ± 0.1. Natural water irradiations were undertaken at the native water pH values, buffered with 10 mM phosphate. The influence of dissolved organic matter (DOM) on oxyhalide analyses and/or formation was investigated by amending phosphate-buffered solutions with SRNOM at a concentration of 2 mg$_C$ L^{-1}, or by using natural waters. A concentration of 200 μg L^{-1} Br$^-$ was added to selected experiments to evaluate formation of BrO$_3^-$ under conditions representative of high-bromide drinking water sources.[75,76]

FAC only and sunlight/FAC experiments were initiated by adding [FAC]$_0$ ~8 mg L^{-1} as Cl$_2$ to the prepared water matrixes in either amber glass reactors or quartz tubes, respectively (see ESI† Text S1 for additional details on experimental procedures). After FAC addition and mixing, samples were quickly (<10 s) collected from each reactor and amended with 0.2 mM EDA to sequester FAC for subsequent measurement of initial oxyhalide concentrations (labeled t = 0). Sunlight/FAC reactors were then placed within the water bath inside of the Atlas solar simulator, whereas FAC only

reactors remained within the water bath located outside of the solar simulator. FAC concentrations were monitored throughout the irradiation or dark reaction periods by means of DPD colorimetry.[70] Sunlight/FAC experimental sets were irradiated for 20 or 45 minutes – equivalent to fluences of 7.2 or 16.1 J cm^{-2} from 290–400 nm (Fig. S2†), as determined using pNA/pyridine actinometry (details provided in Text S2†). Cumulative FAC exposures (CT$_{FAC}$) were determined by trapezoidal Riemann summation of FAC concentrations measured at defined reaction times during the courses of experiments (eqn (8)).

$$\mathrm{CT_{FAC}} = \int_0^t [\mathrm{FAC}]\, dt = \sum \Delta t_i \times \left(\frac{[\mathrm{FAC}]_i + [\mathrm{FAC}]_{i+1}}{2} \right) \quad (8)$$

Dark chlorination experiments proceeded until their cumulative FAC exposures matched the recorded CT$_{FAC}$ of the accompanying 45 minute-irradiated sunlight/FAC samples in paired experiments. To conclude experiments, FAC was sequestered with a two-fold molar excess of EDA.[46,47] Samples were then analyzed for oxyhalide concentrations within 24 hours of collection.

Results and discussion

Method development and optimization

While a wide variety of oxyhalide detection methods are published, available methods typically: (i) enable analyses of only a subset of the oxyhalides most relevant to (waste)water treatment (i.e., ClO$_2^-$, ClO$_3^-$, ClO$_4^-$, BrO$_3^-$, and IO$_3^-$), (ii) require highly-specialized procedures or hardware to achieve sub-μg L^{-1} sensitivities (e.g., on-column pre-concentration, PCR, or suppressed IC-MS instrumentation), and/or (iii) require relatively long run-times per sample (e.g., in excess of 20 minutes) (see Table 1 and associated discussion and references). This work was thus undertaken with the aim of developing a method that would enable rapid (<15 minutes/sample), sub-μg L^{-1} analyses of all five oxyhalides, using conventional LC-MS instrumentation likely to be available in most modern environmental analytical laboratories, with the high chromatographic resolution inherent to IC separations.

Stationary phase and mobile phase selection. A variety of possible chromatography columns were screened for potential use, including a weak anion exchange column (150 × 2 mm, 5 μm, Thermo Scientific Dionex Acclaim® Mixed Mode WAX-1), a C18 column (150 × 2.1 mm, 3 μm, Supelco Ascentis C18), a carbonate-form IC column (250 × 2 mm, 9 μm, Thermo Scientific Dionex IonPac® AS9-HC), and a hydroxide-form IC column (250 × 2 mm, 9 μm, Thermo Scientific Dionex IonPac® AS16). The first three of these were tested using various mobile phases including aqueous ammonium formate, aqueous ammonium acetate, or aqueous ammonium carbonate (WAX-1, C18, AS9-HC), and formic acid with and without methanol or acetonitrile (C18 only), but were in each case found to be inadequate for achieving sufficient separation of the oxyhalides of interest

2584 | Environ. Sci.: Water Res. Technol., 2020, **6**, 2580–2596

This journal is © The Royal Society of Chemistry 2020

within the desired analysis time window. Further testing was therefore undertaken with the hydroxide-form AS16 column.

The AS16 column is recommended for ClO_4^- separation in accordance with U.S. EPA method 314.2 (paired with an AS20 column, for two-dimensional IC-MS) and is also capable of separating a wide variety of polarizable and inorganic anions including ClO_2^- and BrO_3^-, though the AS16 only appears to have been evaluated for these purposes using conventional aqueous KOH or NaOH IC mobile phases and suppressed IC instrumentation.[32,77–79] The reported use of aqueous methylamine in place of KOH or NaOH for LC-MS analysis of ClO_4^- on a Thermo Scientific Dionex AS21 column in U.S. EPA method 331.0 indicated that methylamine could potentially also be used with an AS16 column to provide a source of OH^- without introducing salts that could precipitate or otherwise interfere with ionization in conventional modes of MS analyses. This presented the possibility of using the AS16 column for MS analysis of all five oxyhalides (ClO_2^-, ClO_3^-, ClO_4^-, BrO_3^-, and IO_3^-) without the need for a suppressor.

Initial attempts to use the AS16 column with aqueous methylamine mobile phases failed to achieve acceptable chromatography for each of the oxyhalides, with poor resolution of ClO_2^-, ClO_3^-, and BrO_3^- and excessive retention of ClO_4^- at a representative mobile phase concentration of 200 mM methylamine. Prior work has shown that incorporation of an organic modifier (e.g., methanol, p-cyanophenol, or acetonitrile) into a mobile phase can greatly decrease the retention of ClO_4^- on IC stationary phases, while also improving ClO_4^- peak shape and MS signal intensity (due to more efficient ionization in the ESI chamber).[43,77,78] The use of acetonitrile as a mobile phase modifier was in turn investigated as a means of improving the chromatography and detection of all five oxyhalides. Accordingly, combining aqueous methylamine with a high percentage of acetonitrile as an organic modifier in the mobile phase yielded both rapid elution and improved separation of ClO_2^-, ClO_3^-, ClO_4^-, and BrO_3^- under isocratic conditions. A composition of 20% A (1 M aqueous methylamine) + 80% B (acetonitrile) was found to yield an optimal balance of separation and rapid elution time for these four oxyhalides (Fig. 1 and S3†), though IO_3^- eluted considerably later and with a much broader peak (Fig. S3†). Improvements in IO_3^- chromatography could be achieved under isocratic conditions by lowering the percentage of acetonitrile, though at the expense of diminished separation of the other four oxyhalides (Fig. S3†). As will be discussed below, further modifications to the method were investigated to enable improved IO_3^- chromatography while maintaining the identified optimal conditions for ClO_2^-, ClO_3^-, ClO_4^-, and BrO_3^-.

Influence of mobile phase composition on oxyhalide chromatography. Prior studies and observations from preliminary method development in the present work have shown a typical elution order (in terms of increasing retention times) of $IO_3^- < ClO_2^- < BrO_3^- < ClO_3^- < ClO_4^-$ when using highly aqueous (>90% H_2O) mobile phases with
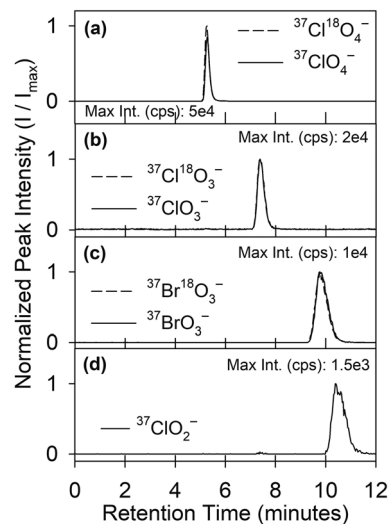

Fig. 1 Extracted ion chromatograms (XICs) for 10 μL injections of (a) ClO_4^-, (b) ClO_3^-, (c) BrO_3^-, and (d) ClO_2^- standards (50 μg L^{-1}) and ^{18}O-isotope internal standards (50 μg L^{-1}) prepared in Milli-Q water, with elution from a 250 × 2 mm, 9 μm, AS16 column using 20% A + 80% B at a flow rate of 0.25 mL min^{-1}.

the AS16 column[27,44] or a Synergi Max-RP C12 column.[49,50] However, as shown in Fig. 1, when employing a highly organic alkaline mobile phase comprising 20% A + 80% B, elution orders for these five oxyhalides were reversed. Other investigators have reported similar reversals of elution order during IC analyses when using mobile phases comprising high organic solvent proportions.[43,58,80,81]

Such trends could be partly due to alterations in analyte ion-mobile phase interactions associated with such analyte ion properties as charge density, hydrophilicity, and polarizability,[82] which may impact the strength of analyte ion interactions at the stationary phase interface during IC analyses.[83,84] Selected properties for ClO_2^-, ClO_3^-, ClO_4^-, BrO_3^-, and IO_3^- (e.g., molecular radius and polarizability, which relate to ion solvation), are summarized in Table 3.[84–88]

Cations and some anions (such as IO_3^-, and to a lesser degree BrO_3^- and ClO_2^-) can be classified as kosmotropes (Table 3) – which are capable of forming stable and organized hydration shells in aqueous solutions – on the basis of their relatively high polarizabilities and dipole moments.[84,87] These stable hydration shells may shield such hydrophilic anions from ion exchange sites and result in their preferential solvation in the bulk solution and early elution within an aqueous mobile phase.[83] In contrast, in a highly organic mobile phase (e.g., ≥80% acetonitrile), the high proportion of organic solvent may disrupt the water hydration shells for such anions, and enhance their interactions with ion exchange sites on the IC stationary phase,[80] consistent with the longer retention times for BrO_3^-, ClO_2^-, and IO_3^- under such conditions (Fig. 1 and S3†). The strong affinity of hydrophilic analytes for the AS16 column media under such conditions could also be responsible for

This journal is © The Royal Society of Chemistry 2020

Environ. Sci.: Water Res. Technol., 2020, 6, 2580–2596 | 2585

Table 3 Summary of oxyhalide anion properties

	Molecular radius[84] (Å)	Polarizability[87] (Å^3)	Dipole moment[87] (D)	Jones–Dole viscosity B coefficient[a,88]	Classification[a,84]
ClO_4^-	2.8	5.4	NA^b	−0.058	Chaotrope
ClO_3^-	2.2	5.1	2.6	−0.022	Chaotrope
ClO_2^-	NA^b	4.9	2.7	0.067	Kosmotrope (loosely hydrated)
BrO_3^-	2.4	6.2	3.6	0.009	Kosmotrope (loosely hydrated)
IO_3^-	3.7	7.4	4.9	0.14	Kosmotrope (strongly hydrated)

^{a} Negative Jones–Dole B coefficients indicative of chaotropic ions, positive Jones–Dole B coefficients indicative of kosmotropic ions.[84] ^{b} NA – Value could not be located in the literature.

the broadening of later eluting analyte peaks apparent in Fig. 1 (most notably for ClO_2^-).

Other anions (such as ClO_4^- and ClO_3^-) can be classified as chaotropes (Table 3), because they disrupt the hydrogen bonding network in water and do not form an ordered hydration shell.[84,89] These less hydrophilic ions are influenced, to a greater degree, by the energy demands associated with cavity formation to accommodate their dissolution in water, which drive chaotropes to aqueous interfacial boundaries, as reported in studies examining ClO_4^- accumulation at air–water interfaces.[84] The relative instability of ClO_4^- in aqueous solutions contributes to its enhanced retention on ion exchange sites and adsorption to stationary phase media (likely driven by van der Waals interactions) when using aqueous KOH or NaOH mobile phases.[27,84] In contrast, ClO_4^- is more amenable to solvation in a mobile phase enriched in an aprotic solvent such as acetonitrile, which hinders its pairing with ion exchange sites and adsorption on to hydrophobic components of the IC stationary phase.[43,80,82] This can in turn provide an explanation for the rapid elution of ClO_4^- from the AS16 stationary phase when using 20% A + 80% B as the mobile phase here.

Influence of acetonitrile on methylamine and stationary phase properties. The observed decrease in ClO_4^- retention and improvements in resolution for the other oxyhalides at higher proportions of acetonitrile could also be partly attributable to an increase in the base strength of the OH$^-$ source – methylamine – when dissolved in a less protic solvent, leading to an effective increase in the available concentration and activity of OH$^-$ for displacement of ions from the AS16 stationary phase (see Text S3† for additional discussion on this point).[90,91] A high proportion of acetonitrile could also inhibit deprotonation of alkanol groups on the AS16 phase (for the same reasons as for methylamine), resulting in increased positive charge density at ion exchange sites and higher propensity for ion-pair interactions of the more hydrophilic analyte ions (e.g., ClO_2^-, BrO_3^-, and IO_3^-) with the stationary phase, as seen in Fig. S3.†[43]

Overall, the above phenomena would be expected to result in enhanced retention of more polarizable, hydrophilic kosmotropic anions that engage with the stationary phase media predominantly by ion-pair formation, such as ClO_2^-,

BrO_3^-, and IO_3^-,[83,87] and decreased retention of less-hydrophilic chaotropic ions, such as ClO_4^- and to a lesser degree ClO_3^-, which form weak ion-pairs and may be solvated to a greater degree than the more hydrophilic anions in mobile phases comprising high proportions of aprotic solvent.[43,80] Taken together, these phenomena can explain the chromatographic behavior observed in Fig. 1 and S3.†

Gradient modification for IO_3^- analysis. As noted above, IO_3^- can be rapidly eluted from the AS16 column under isocratic conditions by operating at a higher aqueous phase proportion (e.g. 35% A + 65% B, as shown in Fig. S3†). Unfortunately, it was not possible to also achieve acceptable chromatography for ClO_2^-, ClO_3^-, ClO_4^-, and BrO_3^- under such conditions (Fig. S3†). However, the described isocratic method can be modified for the analysis of IO_3^- by incorporation of a gradient step following a period of isocratic elution. As demonstrated on LC-MS/MS System 2, after 5.5 minutes of isocratic elution at 20% A + 80% B (i.e., after ClO_3^- elution), the mobile phase was rapidly transitioned to 100% A over a 30 second gradient, then held at a mobile phase composition of 100% A for 5 minutes, and then returned to 20% A + 80% B over a 30 second gradient to equilibrate for 2.5 minutes before the next injection. Under these conditions, IO_3^- eluted rapidly while good separation of the other oxyhalides was also maintained (Fig. S4†).

Limits of detection and quantification. Table 4 summarizes concentration measurements for each oxyhalide over a series of repeated 100 μL injections of individual standards prepared in Milli-Q water, for use in determining the limits of detection (LODs) and limits of quantification (LOQs) for ClO_4^-, ClO_3^-, ClO_2^-, and BrO_3^-. In Table 4, the relative standard deviation (RSD) for each analyzed oxyhalide concentration was calculated as (standard deviation/mean) × 100%. LODs were determined as standard deviation (SD) × Student's (2-sided) t value for a 98% confidence interval with $n − 1 = 7$ degrees of freedom, and LOQs as 3 × LOD.[92] The LOQs for all three oxychlorides were determined to be below 1 μg L^{-1}, with the LOQ of 0.36 μg L^{-1} for ClO_2^- far below the corresponding U.S. EPA MCL of 1.0 mg L^{-1},[12] and the LOQs of 0.06 μg L^{-1} and 0.84 μg L^{-1} for ClO_4^- and ClO_3^- also far below their respective 70 μg L^{-1} and 700 μg L^{-1} WHO drinking water guidelines[93] and relevant provisional U.S. federal or state-level limits.[17] As for the oxychlorides, the

Table 4 NS-IC-MS/MS method sensitivity data for ClO_4^-, ClO_3^-, ClO_2^-, and BrO_3^- ($n = 8$)

Replicate no.	Measured oxyhalide standard concentrations[a] ($\mu g\ L^{-1}$)			
	0.1 $\mu g\ L^{-1}$ ClO_4^-	0.5 $\mu g\ L^{-1}$ ClO_3^-	0.5 $\mu g\ L^{-1}$ ClO_2^-	0.1 $\mu g\ L^{-1}$ BrO_3^-
1	0.13	0.46	0.46	0.08
2	0.13	0.43	0.47	0.11
3	0.12	0.40	0.45	0.11
4	0.13	0.54	0.49	0.11
5	0.11	0.58	0.49	0.09
6	0.12	0.51	0.53	0.09
7	0.13	0.59	0.54	0.10
8	0.13	0.71	0.57	0.11
Mean ($\mu g\ L^{-1}$)	0.12	0.53	0.50	0.10
SD ($\mu g\ L^{-1}$)	0.006	0.093	0.040	0.011
RSD (%)	5.1%	17.8%	7.9%	11.0%
Student's t value (98% CI for $n - 1 = 7$)	2.998	2.998	2.998	2.998
LOD = SD × student's t value ($\mu g\ L^{-1}$)	0.02	0.28	0.12	0.03
LOQ = 3 × LOD ($\mu g\ L^{-1}$)	0.06	0.84	0.36	0.10

[a] LOD and LOQ values are for 100 μL injections of standards prepared in Milli-Q water and eluted from a 250 × 2 mm, 9 μm, AS16 column using 20% A + 80% B at a flow rate of 0.25 mL min⁻¹.

LOQ of 0.10 $\mu g\ L^{-1}$ determined for BrO_3^- is also far below the corresponding U.S. EPA MCL of 10 $\mu g\ L^{-1}$.[12] The LOQs achievable here are consistent with or lower than the range of LOQ values achievable for many other methods (Table 1). IO_3^- quantification in the gradient method was not investigated as extensively as the other four oxyhalides, so its LOQ could only be estimated as <1.0 $\mu g\ L^{-1}$ on the basis of measurements from the isocratic analyses shown in Fig. S3† (using LC-MS/MS System 3). It is anticipated that this could be further lowered with additional optimization of ionization parameters.

Solute and matrix effects on quantification of ClO_4^-, ClO_3^-, ClO_2^-, and BrO_3^- in synthetic and natural waters. Various background ions present in sample matrixes can compete with the oxyhalides for ion exchange sites on stationary phase media; potentially leading to instabilities in analyte retention times. In the present work, high phosphate concentrations (10 mM) in buffered samples were observed to result in progressive decreases in the observed retention times for each oxyhalide with repeated sample injections, as shown in Fig. S5 and in Table S3.† This effect was most pronounced for BrO_3^- and ClO_2^-. In order to address this, precipitation of dissolved phosphate using $Ba(OH)_2$ was investigated. 10 mM phosphate buffered samples were pretreated with 15 mM $Ba(OH)_2$ and mixed for at least 20 minutes to precipitate dissolved phosphate as $Ba_3(PO_4)_{2(s)}$. A sub-set of samples was also adjusted from pH 12 (the pH after $Ba(OH)_2$ addition) to ~pH 8 by addition of H_2SO_4 during the mixing step.

Samples were then filtered through 0.22 μm PTFE membranes (10 mm syringe filters) to retain the $Ba_3(PO_4)_{2(s)}$ precipitate, with filtration in some cases facilitated by initially centrifuging samples at 2000G for 20 minutes to remove larger $Ba_3(PO_4)_{2(s)}$ particles. Final phosphate concentrations were measured with Lovibond™ orthophosphate test tube kits and a Hach spectrometer. Barium precipitation was found to yield full recovery of

spiked oxyhalide concentrations and stable IC retention times after repeated injections (Table S3†). Though not evaluated in this study, sample pretreatment with commercially-available Ba-form ion exchange cartridges would also be expected to be suitable for removal of naturally-occurring concentrations of phosphate.

In order to assess the effects of common water matrix constituents on oxyhalide quantification by the NS-IC-MS/MS method, mixtures of ClO_4^-, ClO_3^-, ClO_2^-, and BrO_3^- (each at 10 $\mu g\ L^{-1}$) were spiked into and quantified within Milli-Q water amended with increasing concentrations of common solutes (i.e., Cl^-, Br^-, HCO_3^-/CO_3^{2-}, SO_4^{2-}, and SRNOM) and within several natural water samples. IO_3^- was not included in these analyses, as it was only incorporated into the method at a later stage of investigation. Fig. 2 illustrates the measured normalized signal intensities for each oxyhalide versus increasing concentrations of Cl^- (0–355 mg L^{-1}), Br^- (0–1 mg L^{-1}), HCO_3^-/CO_3^{2-} (0–10 mM), SO_4^{2-} (0–500 mg L^{-1}), and SRNOM (0–10 mg$_C$ L^{-1}).

Cl^- and Br^- were detected via ESI negative-mode MS Q1 detection (using m/z 34.97 and 36.97 for Cl^-, and m/z 78.91 and 80.91 for Br^-), and found to elute between 9–11 minutes under the isocratic conditions specified for the NS-IC-MS/MS method (using LC-MS/MS System 1). Thus, these common halides would be expected to elute near and possibly alter BrO_3^- and ClO_2^- signal intensities and/or retention times during MS/MS analyses. For reasons currently unknown, increasing concentrations of Cl^- (up to 355 mg L^{-1}) led to an increase in retention time of the BrO_3^- peak (Table S3†), though BrO_3^- signal intensity was unaffected (Fig. 2d). Surprisingly, a similar effect of Cl^- was also observed for ClO_3^- (i.e., increased retention time, no change in signal intensity). While undesirable, the shifts in BrO_3^- and ClO_3^- retention times are nevertheless compensated for by the selectivity of MS/MS detection. In contrast, Cl^- did not appear to affect ClO_2^- retention by the stationary phase (Table S3†), though ClO_2^- signal intensity was observed to decrease as Cl^-
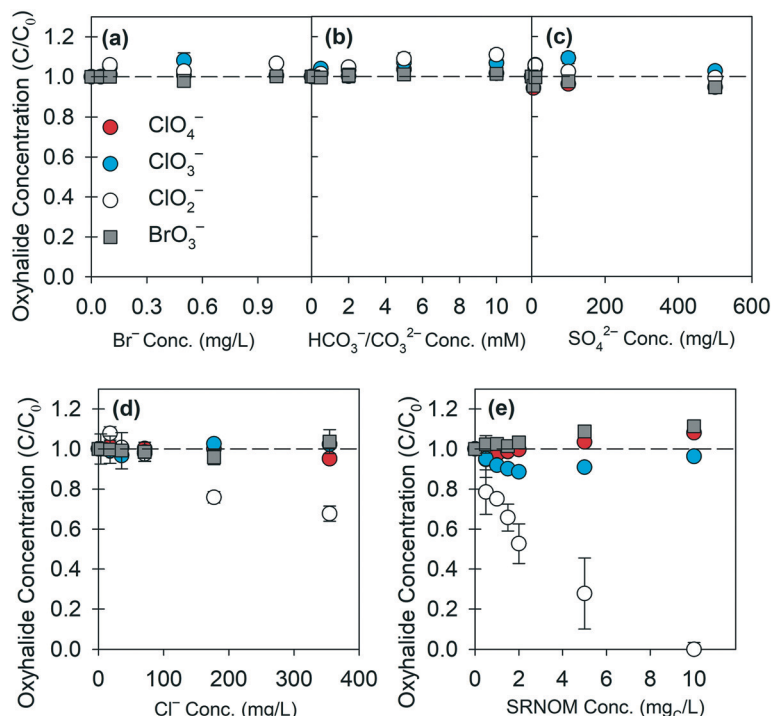
This journal is © The Royal Society of Chemistry 2020

Environ. Sci.: Water Res. Technol., 2020, 6, 2580–2596 | 2587

Fig. 2 Recoveries of oxyhalide standards spiked at 10 μg L^{-1} into Milli-Q water amended with varying concentrations of (a) Br$^-$, (b) HCO$_3^-$/CO$_3^{2-}$, (c) SO$_4^{2-}$, (d) Cl$^-$, and (e) Suwannee River natural organic matter (SRNOM) analyzed using the NS-IC-MS/MS method, with elution from a 250 × 2 mm, 9 μm, AS16 column using 20% A + 80% B at a flow rate of 0.25 mL min^{-1}. Error bars represent one standard deviation about the mean for duplicate samples.

concentration increased to levels >70 mg L^{-1} (Fig. 2d). ClO$_2^-$ and Cl$^-$ elute from the AS16 column at similar times, which may result in suppression of ClO$_2^-$ ionization in the electrospray chamber at higher Cl$^-$ concentrations. While ClO$_2^-$ analyses should be unaffected by Cl$^-$ at levels typical of most drinking waters, Cl$^-$ interference could prove problematic for analysis of ClO$_2^-$ in higher-salinity drinking water matrixes (*e.g.*, groundwaters affected by seawater-intrusion, desalination permeates). Cl$^-$ did not affect either retention times or signal intensities for ClO$_4^-$ (Table S3† and Fig. 2d).

No significant effects of Br$^-$ (up to 1 mg L^{-1}), HCO$_3^-$/CO$_3^{2-}$ (up to 10 mM), or SO$_4^{2-}$ (up to 500 mg L^{-1}) were observed on retention times or signal intensities for ClO$_4^-$, ClO$_3^-$, ClO$_2^-$, or BrO$_3^-$, except perhaps on retention times of BrO$_3^-$ and ClO$_2^-$ at the highest HCO$_3^-$/CO$_3^{2-}$ concentration (10 mM) evaluated (Table S3† and Fig. 2a–c). However, caution may still be warranted in analyses of waters containing very high SO$_4^{2-}$ concentrations, as the ClO$_4^-$ isotopologue (^{35}Cl^{16}O$_4^-$) has a similar mass transition (*m/z* 99 to *m/z* 83, with the loss of one ^{16}O) as two possible isotopologues (H^{34}S^{16}O$_4^-$ and H^{32}S^{16}O$_3^{18}$O$^-$) of HSO$_4^-$,[50,94] which can form during electrospray ionization,[95] indicating the potential for interference of SO$_4^{2-}$ with ClO$_4^-$ analyses under certain circumstances (*e.g.*, in the event that MS/MS detector mass calibrations are not carefully maintained). In such cases, if interference is evident, SO$_4^{2-}$ could potentially be removed from samples by pretreatment with Ba(OH)$_2$ or commercially-available Ba-form ion exchange cartridges.

SRNOM did not have a significant effect on retention times of ClO$_4^-$, ClO$_3^-$, ClO$_2^-$, or BrO$_3^-$, or on the signal intensities of ClO$_4^-$, ClO$_3^-$, or BrO$_3^-$ (Table S3† and Fig. 2e). However, in solutions amended with SRNOM, ClO$_2^-$ signal intensity was observed to decrease even at the lowest added SRNOM concentration of 0.5 mg$_C$ L^{-1} (Fig. 2e), indicating that DOM interference could prove problematic for analysis of ClO$_2^-$ in drinking water matrixes containing appreciable DOC levels. SRNOM could potentially affect the ionization efficiency of ClO$_2^-$ directly, but it may also be reactive toward and reduce the ClO$_2^-$ in spiked samples prior to analysis.[96] It remains unclear whether the observed effect of SRNOM on ClO$_2^-$ analyses is ultimately a consequence of signal suppression, or to direct reaction of ClO$_2^-$ with electron-donating moieties within the SRNOM,[96–98] though prior work suggests that direct reduction of ClO$_2^-$ by NOM may be a minor process.[96] If signal suppression is indeed the primary cause, then use of standard additions to determine ClO$_2^-$ concentrations in high-DOC matrixes could resolve this issue, though at the cost of additional analysis time. These observations suggest that caution may be especially warranted when using the NS-IC-MS/MS method to analyze ClO$_2^-$ in water samples containing elevated DOC concentrations.

As a means of further testing the robustness of the NS-IC-MS/MS method, oxyhalides were quantified in samples of a surface water (obtained from a local reservoir), a treated tap water, and a groundwater from Washington State, as well as in samples of each water spiked with increasing concentrations up to 25 μg L^{-1} of ClO$_4^-$, ClO$_3^-$, ClO$_2^-$, and BrO$_3^-$ (see Table S2†
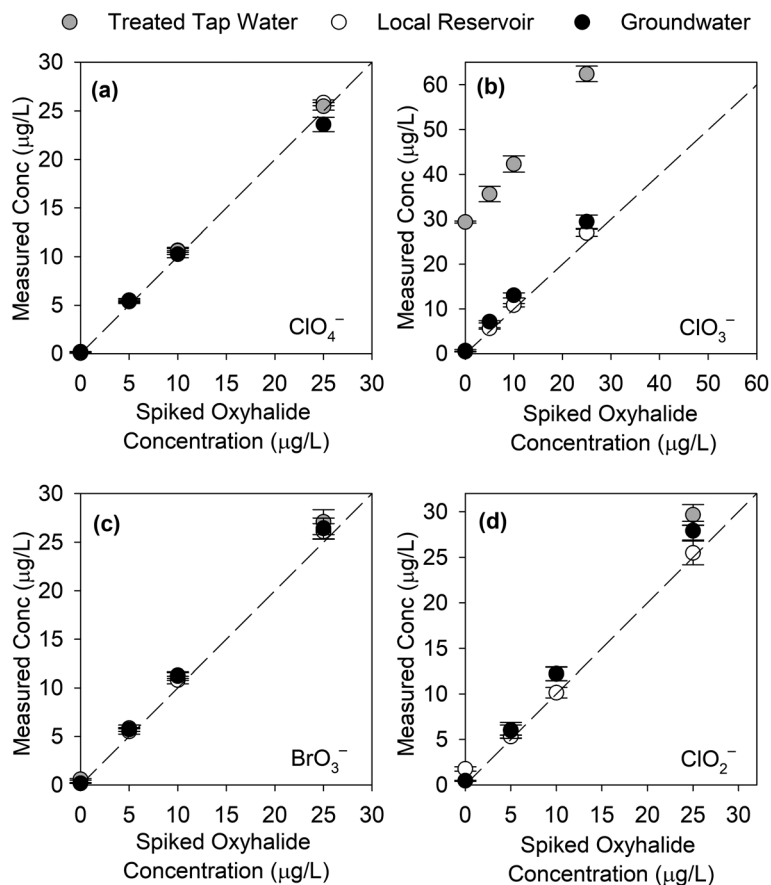
Fig. 3 Measured (a) ClO_4^-, (b) ClO_3^-, (c) BrO_3^-, and (d) ClO_2^- concentrations in spiked and unspiked natural surface water (from a local reservoir), tap water, and a groundwater sample analyzed by NS-IC-MS/MS, with elution from a 250×2 mm, 9 μm, AS16 column using 20% A + 80% B at a flow rate of 0.25 mL min^{-1}. Note that ClO_3^- was detected in the unspiked tap water sample at 29 ± 0.2 μg L^{-1}. Error bars represent one standard deviation about the mean for duplicate samples.

for sample matrix details). Oxyhalides were not detected in any of the unspiked, untreated natural water samples at background levels exceeding 1 μg L^{-1} (Fig. 3), whereas ClO_3^- was measured in the treated tap water sample at a concentration of 29 ± 0.2 μg L^{-1} (most likely as a consequence of formation within NaOCl stocks used by the drinking water utility).[99] As apparent from the linear relationships of measured (*i.e.*, recovered) oxyhalide concentrations *versus* spiked concentrations for each sample, matrix constituents did not appear to have significant effects on stabilities or signal intensities of ClO_4^-, ClO_3^-, ClO_2^-, or BrO_3^-.

Oxyhalide quantification during an advanced oxidation process (sunlight/FAC)

As a means of testing the utility of the NS-IC-MS/MS method for quantifying oxyhalide levels formed during oxidative treatment processes, ClO_4^-, ClO_3^-, ClO_2^-, and BrO_3^- concentrations were monitored during sunlight/FAC treatment under several conditions in 10 mM phosphate buffer and two natural waters (solutions were not amended with or did not otherwise contain appreciable I$^-$ concentrations, so IO_3^- was not monitored). Formation of

oxychlorides and/or BrO_3^- has previously been observed during the UVB, UVA, and simulated sunlight irradiation of FAC-containing solutions or exposure of chlorinated seawater or open chlorinated drinking water reservoirs to natural sunlight,[24,26,67–69] apparently due to the generation of O_3, reactive oxygen species (*e.g.*, $^\bullet$OH), and/or various reactive halogen species (*e.g.*, Cl$^\bullet$, Cl$_2^{\bullet-}$, ClO$^\bullet$, Br$^\bullet$) *via* the photolysis of FAC at sunlight-relevant wavelengths of UVB and UVA light (Table S1† and eqn (1)–(7)).[23,61–63,65] In solutions containing FAC (comprising primarily HOCl/OCl$^-$) and free available bromine (comprising primarily HOBr/OBr$^-$) – formed *via* rapid Br$^-$ oxidation by FAC,[100] reactions involving O_3, as well as reactive oxygen and halogen species such as $^\bullet$OH, Cl$^\bullet$, and Br$^\bullet$, can lead to oxidation of HOCl/OCl$^-$ and HOBr/OBr$^-$ to more highly oxidized forms including ClO_2^-, ClO_3^-, ClO_4^-, and BrO_3^-.[63,64,66,100–102]

Accordingly, in the present work, sunlight/FAC treatment of 10 mM phosphate-buffered solutions was found to yield increased concentrations of ClO_3^- and (with the addition of 200 μg L^{-1} Br$^-$) BrO_3^- (Fig. 4), whereas no formation of either oxyhalide was observed during dark chlorination (FAC only) under the same conditions. Background ClO_3^- and BrO_3^- levels of ~300–400 μg L^{-1} and ~2 μg L^{-1}, respectively,
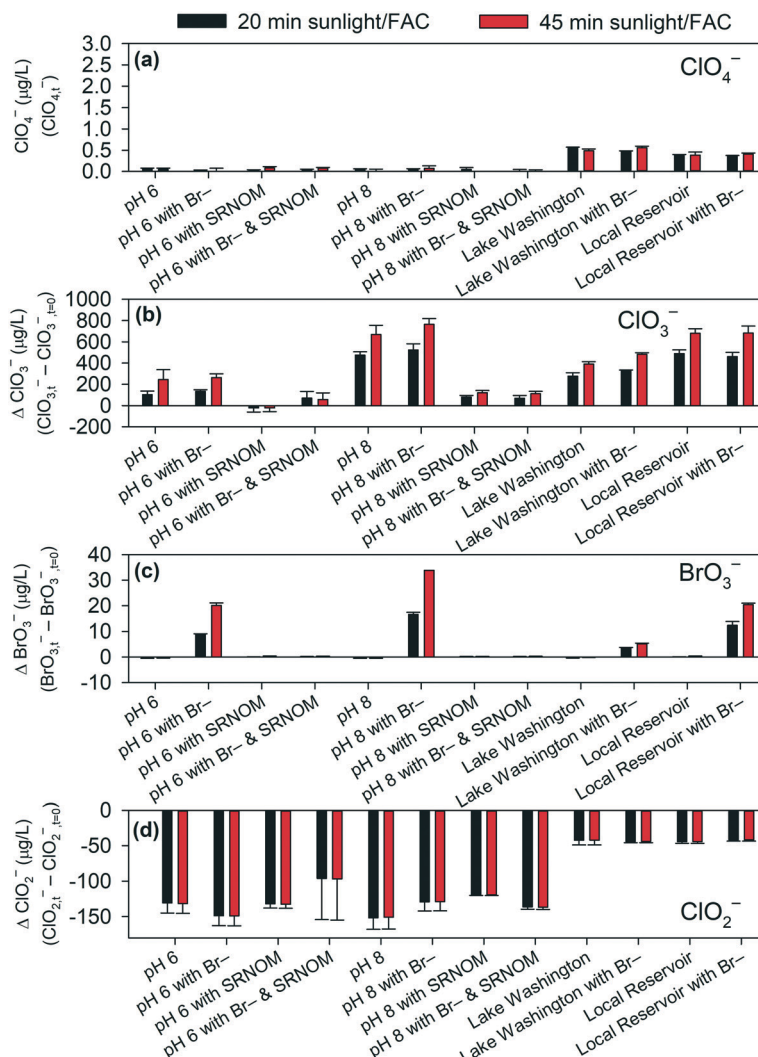
Fig. 4 Concentrations of (a) ClO_4^-, and changes in concentrations (ΔXO_n^-) of (b) ClO_3^-, (c) BrO_3^-, and (d) ClO_2^- in samples subjected to sunlight/FAC treatment. 10 mM phosphate buffer was used to maintain pH in Milli-Q water solutions (pH 6 and 8, with and without 2 mg_C L^{-1} SRNOM) and in natural water samples (adjusted to their native pH of 8.1) at native and fortified Br^- concentrations (where "with Br^-" corresponds to amendment with 200 μg L^{-1} Br^- – in addition to native Br^- levels in natural waters). In sunlight/FAC experiments, samples were irradiated for 20 or 45 minutes (290–400 nm fluence = 7.2 or 16.1 J cm^{-2}). Note that all ΔXO_n^- values were corrected for initial ($t = 0$) background XO_n^- concentrations originating from the NaOCl stock used in preparing FAC solutions (see Fig. S6–S8†). All experiments were conducted at 10 °C, with $[FAC]_0$ ~8 mg L^{-1} as Cl_2. Error bars represent one standard deviation about the mean for duplicate samples.

originated from the NaOCl stock used in preparing FAC solutions – consistent with prior studies,[7,9,11,49,103] with a ~1:26 molar ClO_3^-/FAC ratio and a ~1:10 000 molar BrO_3^-/FAC ratio present in the undiluted NaOCl stock (see Fig. S6–S8†). As shown in Fig. 4, ClO_3^- concentrations up to ~750 μg L^{-1} and BrO_3^- concentrations up to ~35 μg L^{-1} were generated under these conditions, with higher concentrations observed at pH 8 in comparison to pH 6. This highlights that BrO_3^- formation can exceed the U.S. EPA MCL (10 μg L^{-1})[12] and ClO_3^- formation can exceed the WHO guidance level (700 μg L^{-1})[93] in low DOC water with elevated bromide concentrations after >20 minutes of sunlight-driven chlorine photolysis. The apparent pH dependence, which is consistent with that reported for ClO_3^- formation in a prior study,[26] may be due in part to the combination of a higher UV absorbance

and effective quantum yield for O(^{3}P) (and hence O_3) formation at higher pH – due to a shift in speciation toward OCl^- (Fig. S2 and Table S1†).

Interestingly, the presence of DOM (in the form of SRNOM) greatly suppressed formation of both ClO_3^- and BrO_3^- (Fig. 4). This did not appear to be a light screening effect, as FAC photolysis kinetics in SRNOM-containing solutions were actually accelerated compared to those in the absence of SRNOM (Fig. S9†). Furthermore, this did not appear to be due to direct consumption of FAC by SRNOM, as FAC loss rates in the presence of SRNOM in FAC only reactions were much lower than those observed in accompanying sunlight/FAC experiments (Fig. S9†). Rather, the decreased ClO_3^- and BrO_3^- yields and accelerated FAC decay kinetics under these conditions suggest that: (a)

SRNOM directly scavenges reactants involved in the formation of ClO_3^- and BrO_3^-, such as $HOBr/OBr^-$ [104,105] and/or various photogenerated species that may contribute to $HOCl/OCl^-$ or $HOBr/OBr^-$ oxidation (*e.g.*, ˙OH, ˙Cl, or O_3 [24,26,106–108]), and (b) scavenging of photogenerated oxidants by SRNOM initiates and propagates reactions leading to radical chain decomposition of FAC (consistent with prior observations [62,109,110]).

Like ClO_3^-, ClO_2^- was also present in the NaOCl stock used in preparing FAC solutions (at a ~1 : 60 molar ClO_2^-/FAC ratio in the undiluted NaOCl stock – generally consistent with prior studies, [9,11,49,103] yielding background concentrations of ~100–150 μg L^{-1} in FAC solutions; see Fig. S6–S8†). Background ClO_2^- concentrations were completely removed during sunlight/FAC treatment at 290–400 nm fluences >7.2 J cm^{-2} (20 minutes irradiation) (Fig. 4). FAC only experiments both with and without DOM resulted in partial removal of the background ClO_2^- (Fig. S6–S8†), which may be due in part to its slow reaction with $HOCl$, [111] its reaction with electron-rich moieties in the SRNOM, and/or to suppression of its signal intensity in the NS-IC-MS/MS method by the SRNOM. In contrast, the complete loss of ClO_2^- observed during sunlight/FAC treatment is more likely due to rapid oxidation of ClO_2^- by O_3, ROS (*e.g.*, ˙OH), or RHS (*e.g.*, Cl˙, $Cl_2^{˙-}$, or ClO˙). [112,113]

No ClO_4^- formation was detected during FAC only or sunlight/FAC treatment in phosphate buffer under the conditions used in the current work (which employed much lower FAC concentrations than prior work in which ClO_4^- formation was observed during UVB and UVA irradiation) (Fig. 4a). [67,114,115]

Oxyhalide concentrations were also quantified during sunlight/FAC treatment of two surface waters with and without addition of 200 μg L^{-1} Br^-. The two selected water samples included a high-quality surface water (Local Reservoir, in a protected watershed) and an urban-influenced surface water (Lake Washington, located between Seattle, WA and Bellevue, WA). Due to low native Br^- concentrations (Table S2†), BrO_3^- formation was only observed in the sunlight/FAC samples amended with 200 μg L^{-1} Br^- (Fig. 4c), with significantly higher BrO_3^- levels observed in the Local Reservoir sample (20.4 ± 0.5 μg L^{-1} after 45 minutes of irradiation) compared to the Lake Washington sample (5.1 ± 0.3 μg L^{-1} after 45 minutes of irradiation). It is important to note that BrO_3^- formation in the bromide-amended Local Reservoir sample exceeded the U.S. EPA regulatory MCL (10 μg L^{-1}), [12] though the added Br^- concentration is higher than levels encountered in most natural surface waters. [116,117] ClO_3^- formation followed similar trends as BrO_3^-, with ClO_3^- yields of 680 ± 43 μg L^{-1} in the Local Reservoir sample and 390 ± 11 μg L^{-1} in the Lake Washington sample after 45 minutes irradiation during sunlight/FAC treatment without Br^- addition (see Fig. 4b).

In contrast with the sunlight/FAC experiments in phosphate buffer, formation of ClO_3^- during sunlight/FAC treatment remained below the WHO guidance level (700 μg L^{-1}) [93] during sunlight/FAC treatment of the two natural waters (although total ClO_3^- levels did exceed the guidance level when also accounting for background ClO_3^- originating from the NaOCl stock). The higher yields of BrO_3^- and ClO_3^- in the Local Reservoir sample compared to the Lake Washington sample can likely be attributed primarily to the lower DOC concentration in the former (0.5 mg_C L^{-1} *vs.* 2.4 mg_C L^{-1}) – recalling the substantial inhibition of ClO_3^- and BrO_3^- formation by SRNOM during sunlight/FAC treatment (Fig. 4).

As in the cases of phosphate-buffer solutions, initial background ClO_2^- concentrations in each sample (originating from the NaOCl stock used to prepare FAC solutions) were depleted to below LODs during sunlight/FAC treatment. No ClO_4^- formation was observed during sunlight/FAC or FAC only treatment in either water, though low levels (≤0.6 μg L^{-1}) were detected in all of the natural water samples. Analysis of the Local Reservoir sample before modification with any of the reagents added for use in these experiments (*e.g.*, FAC, phosphate buffer, NaOH or H_2SO_4 for pH adjustment, EDA) indicated a native ClO_4^- level of no more than 0.1 μg L^{-1}; thus, at least part of the measured ClO_4^- levels appears likely to have originated as a trace contaminant of the reagents or glassware used for experiments. Although analyses of unmodified Lake Washington water were not undertaken to confirm this, the similar levels of ClO_4^- measured in each matrix indicate a similar explanation for the measured levels of ClO_4^- in the Lake Washington samples.

The preceding observations confirm that during treatment of some waters, sunlight/FAC treatment can generate levels of ClO_3^- and BrO_3^- that exceed recommended guidelines or advisory levels for the former, and the U.S. EPA MCL for the latter. As shown in Fig. 4, formation of ClO_3^- and BrO_3^- during sunlight/FAC treatment is likely to be more substantial in waters that are lower in DOC, higher in Br^-, and have a higher pH. As the greatest benefits in applying the sunlight/FAC process for purposes of improving disinfection of chlorine-resistant microorganisms such as *Cryptosporidium* spp. oocysts and bacterial endospores are realized in waters with lower DOC levels and higher pH, [59,60] it may be desirable to limit potential future applications of this novel treatment approach to waters that contain moderate DOC concentrations (*e.g.*, ~1–2 mg_C L^{-1}), low Br^- concentrations (*e.g.*, <50 μg L^{-1}), and circumneutral to moderately alkaline pH (*e.g.*, pH 7–8) to strike a balance between maximizing microbial inactivation while minimizing formation of oxyhalide DBPs. As demonstrated in previous work, this should also help to minimize formation of regulated halogenated organic DBPs such as trihalomethanes and haloacetic acids. [118] Future work addressing formation of the oxyhalides (including IO_3^-) over a wider range of conditions (*e.g.*, DOC concentrations, Br^- and I^- concentrations, FAC concentrations, pH, temperature) will be necessary to provide further insight into optimal approaches for safe and effective operation of this novel treatment process.

This journal is © The Royal Society of Chemistry 2020

Environ. Sci.: Water Res. Technol., 2020, **6**, 2580–2596 | **2591**

Conclusions

This work demonstrates the utility of a newly-developed non-suppressed ion chromatography–tandem mass spectrometry (NS-IC-MS/MS) method for the rapid, highly-sensitive isocratic analysis of ClO_4^-, ClO_3^-, ClO_2^-, and BrO_3^- in a variety of aqueous matrixes – without the need for prior sample workup or pre-concentration, with the added capability to incorporate a short gradient step for the analysis of IO_3^-. Sample analyses can be completed in less than 15 minutes, with high chromatographic resolution and highly selective detection of ClO_4^-, ClO_3^-, ClO_2^-, and BrO_3^- down to sub-µg L^{-1} limits of quantification, and with the need for relatively low sample volumes (10–100 µL injection volumes are typical). High (10 mM) phosphate concentrations were found to lead to unstable, decreasing retention times for each of the oxyhalides over repeated injections, likely due to competition for ion exchange sites on the AS16 stationary phase, though sample pretreatment with $Ba(OH)_2$ could effectively remove phosphate and eliminate this effect. Caution may be warranted in analyses of ClO_2^- by this approach, as ClO_2^- was found to be susceptible to signal suppression from Cl^-, and either signal suppression or direct reduction by DOM co-occurring in samples. Although SO_4^{2-} has been reported to interfere with ClO_4^- analysis using single-reaction monitoring, the SO_4^{2-} concentrations investigated in this study did not have a discernible effect on ClO_4^- quantification.

The method was validated through the analyses of spiked concentrations of ClO_4^-, ClO_3^-, ClO_2^-, and BrO_3^- in several natural water samples and a treated tap water sample, and was successfully utilized to quantify the formation of up to ~750 µg L^{-1} of ClO_3^- and (when Br^- was present) up to ~35 µg L^{-1} of BrO_3^- during sunlight/FAC treatment in phosphate-buffered reagent water and two natural surface water samples, though the presence of ~2 mg_C L^{-1} of SRNOM in buffered reagent water or native DOM in natural surface waters significantly inhibited formation of both oxyhalides. ClO_2^- originating from the NaOCl used to prepare FAC solutions was partly depleted during dark chlorination experiments, but was completely depleted (presumably by oxidation to ClO_2) by O_3 or various reactive oxygen or halogen species generated during sunlight/FAC treatment in each water matrix. ClO_4^- formation was not observed during sunlight/FAC treatment under any of the investigated conditions.

Overall, the NS-IC-MS/MS method is fast, robust, relatively simple to apply, and sensitive enough to be used for sub-µg L^{-1} quantification of all of the oxyhalides likely to be introduced into treated water from chemical source stocks or formed during conventional and/or advanced oxidative water treatment processes, and – on account of its compatibility with common LC-MS/MS instrumentation – has the potential to greatly expand access to high-sensitivity quantification of ClO_4^-, ClO_3^-, ClO_2^-, BrO_3^-, and IO_3^- beyond the subset of analytical labs equipped with highly-specialized suppressed IC-MS instrumentation.

Conflicts of interest

There are no conflicts of interest to declare.

Acknowledgements

References

1 U. S. EPA, *Alternative Disinfectants and Oxidants Guidance Manual*, United States Environmental Protection Agency, 1999.

2 U. von Gunten, Oxidation processes in water treatment: are we on track?, *Environ. Sci. Technol.*, 2018, **52**(9), 5062–5075.

3 U. von Gunten, Ozonation of drinking water: Part II. Disinfection and by-product formation in presence of bromide, iodide, or chloride, *Water Res.*, 2003, **37**, 1469–1487.

4 E. M. Aieta and J. D. Berg, A review of chlorine dioxide in drinking-water treatment, *J. - Am. Water Works Assoc.*, 1986, **78**(6), 62–72.

5 K. Alfredo, B. Stanford, J. A. Roberson and A. Eaton, Chlorate challenges for water systems, *J. - Am. Water Works Assoc.*, 2015, **107**(4), E187–E196.

6 AWWA, *2017 Water Utility Disinfection Survey Report*, American Water Works Association, 2018.

7 B. D. Stanford, A. N. Pisarenko, D. J. Dryer, J. C. Zeigler-Holady and S. Gamage, *et al.* Chlorate, perchlorate, and bromate in onsite-generated hypochlorite systems, *J. - Am. Water Works Assoc.*, 2013, **105**(3), E93–E102.

8 R. Aranda-Rodriguez, F. Lemieux, Z. Y. Jin, J. Hnatiw and A. M. Tugulea, (Yet more) challenges for water treatment plants: potential contribution of hypochlorite solutions to bromate, chlorate, chlorite and perchlorate in drinking water, *J. Water Supply: Res. Technol. – AQUA*, 2017, **66**(8), 621–631.

9 R. J. Garcia-Villanova, M. V. O. D. Leite, J. M. Hernandez-Hierro, S. D. Alfageme and C. G. Hernandez, Occurrence of bromate, chlorite and chlorate in drinking waters disinfected with hypochlorite reagents. Tracing their origins, *Sci. Total Environ.*, 2010, **408**(12), 2616–2620.

10 G. Gordon, L. C. Adam, B. P. Bubnis, C. Kuo and R. S. Cushing, *et al.* Predicting liquid bleach decomposition, *J. - Am. Water Works Assoc.*, 1997, **89**(4), 142–149.

11 M. Bolyard, P. S. Fair and D. P. Hautman, Occurrence of chlorate in hypochlorite solutions used for drinking water disinfection, *Environ. Sci. Technol.*, 1992, **26**(8), 1663–1665.

12 U. S. EPA, *National Primary Drinking Water Regulations*, 2020, [Available from: https://www.epa.gov/ground-water-and-drinking-water/national-primary-drinking-water-regulations.

13 Y. Kurokawa, Y. Hayashi, A. Maekawa, M. Takahashi and T. Kokubo, *et al.* Carcinogenicity of Potassium Bromate Administered Orally to F344 Rats, *J. Natl. Cancer Inst.*, 1983, **71**(5), 965–972.

14 D. Couri, M. S. Abdelrahman and R. J. Bull, Toxicological Effects of Chlorine Dioxide, Chlorite and Chlorate, *Environ. Health Perspect.*, 1982, **46**, 13–17.

15 U. S. EPA, *Six-Year Review 3 Technical Support Document for Chlorate*, Office of Water, Cincinnati, OH, 2016.

16 C. Steffen and E. Wetzel, Chlorate Poisoning - Mechanism of Toxicity, *Toxicology*, 1993, **84**(1–3), 217–231.

17 U. S. EPA, *Perchlorate in Drinking Water: Proposed Rule*, 2019, [Available from: https://www.epa.gov/sdwa/perchlorate-drinking-water#main-content.

18 J. C. Siglin, D. R. Mattie, D. E. Dodd, P. K. Hildebrandt and W. H. Baker, A 90-day drinking water toxicity study in rats of the environmental contaminant ammonium perchlorate, *Toxicol. Sci.*, 2000, **57**(1), 61–74.

19 D. Wang, J. R. Bolton, S. A. Andrews and R. Hofmann, Formation of disinfection by-products in the ultraviolet/chlorine advanced oxidation process, *Sci. Total Environ.*, 2015, **518**, 49–57.

20 Y.-H. Chuang, S. Chen, C. J. Chinn and W. A. Mitch, Comparing the UV/monochloramine and UV/free chlorine advanced oxidation processes (AOPs) to the UV/hydrogen peroxide AOP under scenarios relevant to potable reuse, *Environ. Sci. Technol.*, 2017, **51**(23), 13859–13868.

21 W. Li, T. Jain, K. Ishida, C. K. Remucal and H. Liu, A mechanistic understanding of the degradation of trace organic contaminants by UV/hydrogen peroxide, UV/persulfate and UV/free chlorine for water reuse, *Environ. Sci.: Water Res. Technol.*, 2017, **3**(1), 128–138.

22 C. Remucal and D. Manley, Emerging investigators series: the efficacy of chlorine photolysis as an advanced oxidation process for drinking water treatment, *Environ. Sci.: Water Res. Technol.*, 2016, **2**(4), 565–579.

23 D. M. Bulman, S. P. Mezyk and C. K. Remucal, The impact of pH and irradiation wavelength on the production of reactive oxidants during chlorine photolysis, *Environ. Sci. Technol.*, 2019, **53**(8), 4450–4459.

24 X. Zhang, J. He, Y. Lei, Z. Qiu and S. Cheng, *et al.* Combining solar irradiation with chlorination enhances the photochemical decomposition of microcystin-LR, *Water Res.*, 2019, **159**, 324–332.

25 P. Sun, W.-N. Lee, R. Zhang and C.-H. Huang, Degradation of DEET and caffeine under UV/chlorine and simulated sunlight/chlorine conditions, *Environ. Sci. Technol.*, 2016, **50**(24), 13265–13273.

26 S. Cheng, X. Zhang, W. Song, Y. Pan and D. Lambropoulou, *et al.* Photochemical oxidation of PPCPs using a

combination of solar irradiation and free available chlorine, *Sci. Total Environ.*, 2019, **682**, 629–638.

27 E. S. Gilchrist, D. A. Healy, V. N. Morris and J. D. Glennon, A review of oxyhalide disinfection byproducts determination in water by ion chromatography and ion chromatography-mass spectroscopy, *Anal. Chim. Acta*, 2016, **942**, 12–22.

28 Y. Bichsel, *Behavior of Iodine Species in Oxidative Processes During Drinking Water Treatment*, Swiss Federal Institute of Technology Zurich, Zurich, Switzerland, 2000.

29 E. Salhi and U. von Gunten, Simultaneous determination of bromide, bromate and nitrite in low $\mu g \; L^{-1}$ levels by ion chromatography without sample pretreatment, *Water Res.*, 1999, **33**(15), 3239–3244.

30 U. S. EPA, *Method 302.0: Determination of Bromate in Drinking Water using Two-dimensional Ion Chromatography with Suppressed Conductivity Detection*, Cincinnati, OH, 2009.

31 U. S. EPA, *Method 326.0: Determination of Iorganic Oxyhalide Disinfection By-products in Drinking Water using Ion Chromatography Incorporating the Addition of a Suppressor Acidified Postcolumn Reagent for Trace Bromate Analysis*, Cincinnati, OH, 2002.

32 U. S. EPA, *Method 314.2: Determination of perchlorate in drinking water using two-dimensional ion chromatography with suppressed conductivity detection*, Cincinnati, OH, 2008.

33 D. P. Hautman, D. J. Munch, C. Frebis, H. P. Wagner and B. V. Pepich, Review of the methods of the US Environmental Protection Agency for bromate determination and validation of Method 317.0 for disinfection by-product anoins and low-level bromate, *J. Chromatogr. A*, 2001, **920**, 221–229.

34 H. P. Wagner, B. V. Pepich, D. P. Hautman and D. J. Munch, US Environmental Protection Agency Method 326.0, a new method for monitoring inorganic oxyhalides and optimization of the postcolumn derivatization for the selective determination of trace levels of bromate, *J. Chromatogr. A*, 2002, **956**, 93–101.

35 R. J. Joyce and H. S. Dhillon, Trace level determination of bromate in ozonated drinking water using ion chromatography, *J. Chromatogr. A*, 1994, **671**, 165–171.

36 H. S. Weinberg, H. Yamada and R. J. Joyce, New, sensitive and selective method for determining sub-$\mu g/l$ levels of bromate in drinking water, *J. Chromatogr. A*, 1998, **804**(1–2), 137–142.

37 B. Zhu, Z. Zhong and J. Yao, Ion chromatographic determination of trace iodate, chlorite, chlorate, bromate, and nitrite in drinking water using suppressed conductivity detection in visible detection, *J. Chromatogr. A*, 2006, **1118**, 106–110.

38 B. Nowack and U. von Gunten, Determination of chlorate at low $\mu g/l$ levels by ion-chromatography with postcolumn reaction, *J. Chromatogr. A*, 1999, **849**, 209–215.

39 U. S. EPA, *Method 332.0: Determination of perchlorate in drinking water by ion chromatography with suppressed conductivity and electrospray ionization mass spectrometry*, Cincinnati, OH, 2005.

40 H. El Aribi, Y. J. C. Le Blanc, S. Antonsen and T. Sakuma, Analysis of perchlorate in foods and beverages by ion

This journal is © The Royal Society of Chemistry 2020

Environ. Sci.: Water Res. Technol., 2020, **6**, 2580–2596 | **2593**

chromatography coupled with tandem mass spectrometry (IC-ESI-MS/MS), *Anal. Chim. Acta*, 2006, **567**, 39–47.

41 U. S. EPA, *Method 557: Determination of haloacetic acids, bromate, and dalapon in drinking water by ion chromatography electrospray ionization tandem mass spectrometry (IC-ESI-MS/MS)*, Cincinnati, OH, 2009.

42 S. Cavalli, S. Polesello and S. Valsecchi, Chloride interference in the determination of bromate in drinking water by reagent free ion chromatography with mass spectrometry detection, *J. Chromatogr. A*, 2005, **1085**, 42–46.

43 E. S. Gilchrist, P. N. Nesterenko, N. W. Smith and L. P. Barron, Organic solvent and temperature-enhanced ion chromatography-high resolution mass spectrometry for the determination of low molecular weight organic and inorganic anions, *Anal. Chim. Acta*, 2015, **865**, 83–91.

44 L. Barron and B. Paull, Simultaneous determination of trace oxyhalides and haloacetic acids using suppressed ion chromatography-electrospray mass spectrometry, *Talanta*, 2006, **69**(3), 621–630.

45 S. Wu, T. Anumol, J. Gandhi and S. A. Snyder, Analysis of haloacetic acids, bromate, and dalapon in natural waters by ion chromatography–tandem mass spectrometry, *J. Chromatogr. A*, 2017, **1487**, 100–107.

46 U. S. EPA, *Method 300.1: Determination of Inorganic Anions in Drinking Water by Ion Chromatography*, Cincinnati, OH, 1997.

47 U. S. EPA, *Method 317.0: Determination of Inorganic Oxyhalide Disinfection By-products in Drinking Water Using Ion Chromatography with the Addition of a Postcolumn reagent for the Trace Bromate Analysis*, Cincinnati, OH, 2001.

48 Y. Bichsel and U. Von Gunten, Determination of iodide and iodate by ion chromatography with postcolumn reaction and UV/visible detection, *Anal. Chem.*, 1999, **71**(1), 34–38.

49 A. N. Pisarenko, B. D. Stanford, O. Quinones, G. E. Pacey and G. Gordon, *et al.* Rapid analysis of perchlorate, chlorate and bromate ions in concentrated sodium hypochlorite solutions, *Anal. Chim. Acta*, 2010, **659**(1–2), 216–223.

50 S. A. Snyder, B. J. Vanderford and D. J. Rexing, Trace analysis of bromate, chlorate, iodate, and perchlorate in natural and bottled waters, *Environ. Sci. Technol.*, 2005, **39**(12), 4586–4593.

51 U. S. EPA, *Method 331.0: Determination of perchlorate in drinking water by liquid chromatography electrospray ionization mass spectrometry*, Cincinnati, OH, 2005.

52 D. M. West, R. Mu, S. Gamagedara, Y. Ma and C. Adams, *et al.* Simultaneous detection of perchlorate and bromate using rapid high-performance ion exchange chromatography - tandem mass spectrometry and perchlorate removal in drinking water, *Environ. Sci. Pollut. Res.*, 2015, **22**, 8594–8602.

53 R. Xue, A. Donovan, H. Shi, J. Yang and B. Hua, *et al.* Rapid simultaneous analysis of 17 haloacetic acids and related halogenated water contaminants by high-performance ion chromatography-tandem mass spectrometry, *Anal. Bioanal. Chem.*, 2016, **408**(24), 6613–6622.

54 R. T. Wilkin, D. D. Fine and N. G. Burnett, Perchlorate behavior in a municipal lake following fireworks displays, *Environ. Sci. Technol.*, 2007, **41**, 3966–3971.

55 H. L. Shi and C. Adams, Rapid IC-ICP/MS method for simultaneous analysis of iodoacetic acids, bromoacetic acids, bromate, and other related halogenated compounds in water, *Talanta*, 2009, **79**(2), 523–527.

56 Q. Wu, T. Zhang, H. Sun and K. Kannan, Perchlorate in tap water, groundwater, surface waters, and bottled water from China and its association with other inorganic anions and with disinfection byproducts, *Arch. Environ. Contam. Toxicol.*, 2010, **58**, 543–550.

57 L. Charles and D. Pepin, Electrospray ion chromatography tandem mass spectrometry of oxyhalides at sub-ppb levels, *Anal. Chem.*, 1998, **70**(2), 353–359.

58 W. Buchberger and K. Haider, Studies on the combination of ion chromatography-particle-beam mass spectrometry with capillary columns, *J. Chromatogr. A*, 1997, **770**(1), 59–68.

59 J. E. Forsyth, P. R. Zhou, Q. X. Mao, S. S. Asato and J. S. Meschke, *et al.* Enhanced Inactivation of Bacillus subtilis Spores during Solar Photolysis of Free Available Chlorine, *Environ. Sci. Technol.*, 2013, **47**(22), 12976–12984.

60 P. Zhou, G. D. Di Giovanni, J. S. Meschke and M. C. Dodd, Enhanced inactivation of Cryptosporidium parvum oocysts during solar photolysis of free available chlorine, *Environ. Sci. Technol. Lett.*, 2014, **1**(11), 453–458.

61 L. H. Nowell and J. Hoigne, Photolysis of Aqueous Chlorine at Sunlight and Ultraviolet Wavelengths. 2. Hydroxyl Radical Production, *Water Res.*, 1992, **26**(5), 599–605.

62 B. G. Oliver and J. H. Carey, Photochemical Production of Chlorinated Organics in Aqueous-Solutions Containing Chlorine, *Environ. Sci. Technol.*, 1977, **11**(9), 893–895.

63 G. V. Buxton and M. S. Subhani, Radiation chemistry and photochemistry of oxychlorine ions. Part 1.—Radiolysis of aqueous solutions of hypochlorite and chlorite ions, *J. Chem. Soc., Faraday Trans. 1*, 1972, **68**, 947–957.

64 G. V. Buxton and M. S. Subhani, Radiation chemistry and photochemistry of oxychlorine ions. Part 2.— Photodecomposition of aqueous solutions of hypochlorite ions, *J. Chem. Soc., Faraday Trans. 1*, 1972, **68**, 958–969.

65 G. V. Buxton, C. L. Greenstock, W. P. Helman and A. B. Ross, Critical Review of Rate Constants for Reactions of Hydrated Electrons, Hydrogen Atoms and Hydroxyl Radicals ($\cdot$OH/O$\cdot^-$) in Aqueous Solution, *J. Phys. Chem. Ref. Data*, 1988, **17**(2), 513–886.

66 U. von Gunten and Y. Oliveras, Advanced Oxidation of Bromide-Containing Waters - Bromate Formation Mechanisms, *Environ. Sci. Technol.*, 1998, **32**, 63–70.

67 B. Rao, N. Estrada, S. McGee, J. Mangold and B. Gu, *et al.* Perchlorate Production by Photodecomposition of Aqueous Chlorine Solutions, *Environ. Sci. Technol.*, 2012, **46**(21), 11635–11643.

68 D. L. Macalady, J. H. Carpenter and C. A. Moore, Sunlight-Induced Bromate Formation in Chlorinated Seawater, *Science*, 1977, **195**(4284), 1335–1337.

69 C. Tomerlin, Made in the Shade, *Opflow*, 2008, **34**(8), 10–13.

70 APHA/AWWA/WEF, *Standard Methods: 4500-Cl G. DPD Colorimetric Method*, American Public Health Association, Washington D.C., 22nd edn, 2012.

71 M. Bolyard, P. S. Fair and D. P. Hautman, Sources of chlorate ion in US drinking water, *J. - Am. Water Works Assoc.*, 1993, **85**(9), 81–88.

72 D. P. Hautman and M. Bolyard, Using ion chromatography to analyze inorganic disinfection by-products, *J. - Am. Water Works Assoc.*, 1992, **84**(11), 88–93.

73 D. P. Hautman and M. Bolyard, Analysis of oxyhalide disinfection by-products and other anions of interest in drinking water by ion chromatography, *J. Chromatogr.*, 1992, **602**(1–2), 65–74.

74 D. A. Buckingham, F. R. Keene and A. M. Sargeson, Base Hydrolysis of Coordinated Acetonitrile, *J. Am. Chem. Soc.*, 1973, **95**(17), 5649–5652.

75 *ICR auxiliary 1 database version 5.0, query tool version 2.0 [Internet]*, US Environmental Protection Agency, 2000, [cited May 31, 2019], Available from: https://www.epa.gov/dwsixyearreview/supplemental-data-six-year-review-3.

76 R. S. Magazinovic, B. C. Nicholson, D. E. Mulcahy and D. E. Davey, Bromide levels in natural waters: its relationship to levels of both chloride and total dissolved solids and the implications for water treatment, *Chemosphere*, 2004, **57**(4), 329–335.

77 P. E. Jackson, M. Laikhtman and J. S. Rohrer, Determination of trace level perchlorate in drinking water and ground water by ion chromatography, *J. Chromatogr. A*, 1999, **850**(1–2), 131–135.

78 P. E. Jackson, S. Gokhale, T. Streib, J. S. Rohrer and C. A. Pohl, Improved method for the determination of trace perchlorate in ground and drinking waters by ion chromatography, *J. Chromatogr. A*, 2000, **888**(1–2), 151–158.

79 Thermo Scientific, *Dionex IonPac AS16 Column Product Manual*, 2012.

80 T. Okada, Nonaqueous anion-exchange chromatography I. Role of solvation in anion-exchange resin, *J. Chromatogr. A*, 1997, **758**(1), 19–28.

81 P. J. Dumont and J. S. Fritz, Ion chromatographic separation of alkali metals in organic solvents, *J. Chromatogr. A*, 1995, **706**(1), 149–158.

82 S. Rabin and J. Stillian, Practical Aspects on the Use of Organic-Solvents in Ion Chromatography, *J. Chromatogr. A*, 1994, **671**(1–2), 63–71.

83 T. Okada, Interpretation of chromatographic behavior of ions based on the electric double-layer theory, *J. Chromatogr. A*, 1999, **850**(1–2), 3–8.

84 A. P. dos Santos, A. Diehl and Y. Levin, Surface tensions, surface potentials, and the Hofmeister series of electrolyte solutions, *Langmuir*, 2010, **26**(13), 10778–10783.

85 H. H. Eysel, Raman intensities of liquids: absolute scattering activities and Cl-O bond EOPs of ClO−, ClO2−, ClO3- and ClO4- ions in aqueous solution, *Spectrochim. Acta, Part A*, 1988, **44**(10), 991–997.

86 H. H. Eysel, K.-G. Lipponer, C. Oberle and I. Zahn, Raman intensities of liquids: Absolute scattering activities and electro-optical parameters of the halate ions ClO3−, BrO3−, and IO3− in aqueous solutions, *Spectrochim. Acta, Part A*, 1992, **48**(2), 219–224.

87 C. Oberle and H. H. Eysel, Ab initio calculations for some oxo-anions of chlorine, bromine and iodine, *J. Mol. Struct.: THEOCHEM*, 1993, **280**(1), 107–115.

88 H. D. B. Jenkins and Y. Marcus, Viscosity B-Coefficients of Ions in Solution, *Chem. Rev.*, 1995, **95**(8), 2695–2724.

89 P. L. Nostro, B. W. Ninham, S. Milani, A. L. Nostro and G. Pesavento, *et al.* Hofmeister effects in supramolecular and biological systems, *Biophys. Chem.*, 2006, **124**(3), 208–213.

90 E. Rossini, A. D. Bochevarov and E. W. Knapp, Empirical Conversion of pKa Values between Different Solvents and Interpretation of the Parameters: Application to Water, Acetonitrile, Dimethyl Sulfoxide, and Methanol, *ACS Omega*, 2018, **3**(2), 1653–1662.

91 S. Espinosa, E. Bosch and M. Roses, Retention of ionizable compounds in high-performance liquid chromatography: 14. Acid–base pK values in acetonitrile–water mobile phases, *J. Chromatogr. A*, 2002, **964**(1–2), 55–66.

92 L. A. Currie, Nomenclature in evaluation of analytical methods including detection and quantification capabilities (IUPAC Recommendations 1995), *Pure Appl. Chem.*, 1995, **67**(10), 1699–1723.

93 World Health Organization, *Guidelines for drinking water quality: Fourth edition incorporating first addendum*, Geneva, 2017.

94 Y. Li and E. J. George, Analysis of perchlorate in water by reversed-phase LC/ESI-MS/MS using an internal standard technique, *Anal. Chem.*, 2005, **77**(14), 4453–4458.

95 A. T. Blades and P. Kebarle, Study of the Stability and Hydration of Doubly Charged Ions in the Gas Phase: SO42-, S2O62-, S2O82-, and Some Related Species, *J. Am. Chem. Soc.*, 1994, **116**(23), 10761–10766.

96 W. Gan, S. Huang, Y. Ge, T. Bond and P. Westerhoff, *et al.* Chlorite formation during ClO2 oxidation of model compounds having various functional groups and humic substances, *Water Res.*, 2019, **159**, 348–357.

97 M. Aeschbacher, M. Sander and R. P. Schwarzenbach, Novel Electrochemical Approach to Assess the Redox Properties of Humic Substances, *Environ. Sci. Technol.*, 2010, **44**, 87–93.

98 L. Önnby, N. Walpen, E. Salhi, M. Sander and U. von Gunten, Two analytical approaches quantifying the electron donating capacities of dissolved organic matter to monitor its oxidation during chlorination and ozonation, *Water Res.*, 2018, **44**, 677–689.

99 B. D. Stanford, Perchlorate, Bromate, and Chlorate in Hypochlorite Solutions: Guidelines for Utilities (vol 103, pg 71, 2011), *J. - Am. Water Works Assoc.*, 2011, **103**(8), 100.

100 M. Deborde and U. R. S. Von Gunten, Reactions of chlorine with inorganic and organic compounds during water treatment—kinetics and mechanisms: a critical review, *Water Res.*, 2008, **42**(1–2), 13–51.

101 D. Zehavi and J. Rabani, Oxidation of aqueous bromide ions by hydroxyl radicals. Pulse radiolytic investigation, *J. Phys. Chem.*, 1972, **76**(3), 312–319.

102 U. Pinkernell and U. von Gunten, Bromate minimization during ozonation: Mechanistic considerations, *Environ. Sci. Technol.*, 2001, **35**(12), 2525–2531.

103 L. C. Adam and G. Gordon, Hypochlorite ion decomposition: effects of temperature, ionic strength, and chloride ion, *Inorg. Chem.*, 1999, **38**(6), 1299–1304.

104 G. Hua, D. A. Reckhow and J. Kim, Effect of bromide and iodide ions on the formation and speciation of disinfection byproducts during chlorination, *Environ. Sci. Technol.*, 2006, **40**(9), 3050–3056.

105 M. B. Heeb, J. Criquet, S. G. Zimmermann-Steffens and U. Von Gunten, Oxidative treatment of bromide-containing waters: formation of bromine and its reactions with inorganic and organic compounds—a critical review, *Water Res.*, 2014, **48**, 15–42.

106 I. A. Ike, T. Karanfil, J. Cho and J. Hur, Oxidation byproducts from the degradation of dissolved organic matter by advanced oxidation processes–A critical review, *Water Res.*, 2019, 114929.

107 P. Westerhoff, S. P. Mezyk, W. J. Cooper and D. Minakata, Electron pulse radiolysis determination of hydroxyl radical rate constants with Suwannee river fulvic acid and other dissolved organic matter isolates, *Environ. Sci. Technol.*, 2007, **41**(13), 4640–4646.

108 L. Varanasi, E. Coscarelli, M. Khaksari, L. R. Mazzoleni and D. Minakata, Transformations of dissolved organic matter induced by UV photolysis, hydroxyl radicals, chlorine radicals, and sulfate radicals in aqueous-phase UV-based advanced oxidation processes, *Water Res.*, 2018, **135**, 22–30.

109 J. Jin, M. G. El-Din and J. R. Bolton, Assessment of the UV/Chlorine process as an advanced oxidation process, *Water Res.*, 2011, **45**, 1890–1896.

110 Y. Feng, D. W. Smith and J. R. Bolton, Photolysis of aqueous free chlorine species (HOCl and OCl) with 254 nm ultraviolet light, *J. Environ. Eng. Sci.*, 2007, **6**(3), 277–284.

111 Z. Jia, D. W. Margerum and J. S. Francisco, General-acid-catalyzed reactions of hypochlorous acid and acetyl hypochlorite with chlorite ion, *Inorg. Chem.*, 2000, **39**, 2614–2620.

112 U. K. Klaning, K. Sehested and J. Holeman, Standard Gibbs energy of formation of the hydroxyl radical in aqueous solution, *J. Phys. Chem.*, 1985, **89**, 760–763.

113 Z. B. Alfassi, R. E. Huie, S. Mosseri and P. Neta, Kinetics of one-electron oxidation by the ClO radical, *Int. J. Radiat. Appl. Instrum., Part C*, 1988, **32**(1), 85–88.

114 N. Kang, T. A. Anderson and W. Andrew Jackson, Photochemical formation of perchlorate from aqueous oxychlorine anions, *Anal. Chim. Acta*, 2006, **567**(1), 48–56.

115 G. V. Buxton and M. S. Subhani, Radiation-chemistry and photochemistry of oxychlorine ions. 3. Photodecomposition of aqueous-solutions of chlorite ions, *J. Chem. Soc., Faraday Trans. 1*, 1972, **68**, 970–977.

116 U. S. EPA, *ICR auxiliary 1 database version 5.0, query tool version 2.0*, 2000.

117 U. von Gunten and E. Salhi, Bromate in drinking water a problem in Switzerland?, *Ozone: Sci. Eng.*, 2003, **25**(3), 159–166.

118 T. R. Young, W. Li, A. Guo, G. Korshin and M. C. Dodd, Characterization of disinfection byproduct formation and associated changes to dissolved organic matter during solar chlorine photolysis of free available chlorine, *Water Res.*, 2018, **146**(1), 318–327.